Contents lists available at ScienceDirect

Chemosphere

journal homepage: http://ees.elsevier.com

Characteristics of chemical profile, sources and PAH toxicity of $PM_{2.5}$ in beijing in autumn-winter transit season with regard to domestic heating, pollution control measures and meteorology

Fengxia Li [a,1], Jianwei Gu [b,1], Jinyuan Xin [c,d,**], Juergen Schnelle-Kreis [a,*], Yuesi Wang [c], Zirui Liu [c], Rongrong Shen [c], Bernhard Michalke [e], Guelcin Abbaszade [a], Ralf Zimmermann [a]

[a] Joint Mass Spectrometry Center, Cooperation Group Comprehensive Molecular Analytics, Helmholtz Zentrum München, Neuherberg, Germany
[b] Institute of Environmental Health and Pollution Control, School of Environmental Science and Engineering, Guangdong University of Technology, Guangzhou, China
[c] State Key Laboratory of Atmospheric Boundary Layer Physics and Atmospheric Chemistry, Institute of Atmospheric Physics, Chinese Academy of Sciences, Beijing, China
[d] Collaborative Innovation Center on Forecast and Evaluation of Meteorological Disasters, Nanjing University of Information Science & Technology, Nanjing, China
[e] Research Unit Analytical BioGeoChemistry, Helmholtz Zentrum München, Neuherberg, Germany

ARTICLE INFO

Article history:
Received 30 September 2020
Received in revised form 22 February 2021
Accepted 26 February 2021
Available online xxx
Handling Editor: R Ebinghaus

Keywords
$PM_{2.5}$
Air pollution
Chemical composition
Positive matrix factorization
BaP_{eq}
Beijing

ABSTRACT

Several air pollution episodes occurred in Beijing before and after the 2014 Asia-Pacific Economic Cooperation (APEC) summit, during which air-pollution control measures were implemented. Within this autumn-winter transit season, domestic heating started. Such interesting period merits comprehensive chemical characterization, particularly the organic species, to look into the influence of additional heating sources and the control measures on air pollution. Therefore, this study performed daily and 6h time resolved $PM_{2.5}$ sampling from the 24th October to 7th December, 2014, followed by comprehensive chemical analyses including water-soluble ions, elements and organic source-markers. Apparent alterations of chemical profiles were observed with the initiation of domestic heating. Through positive matrix factorization (PMF) source apportionment modeling, six $PM_{2.5}$ sources including secondary inorganic aerosol (SIA), traffic emission, coal combustion, industry emission, biomass burning and dust were separated and identified. Coal combustion was successfully distinguished from traffic emission by hopane diagnostic ratio. The result of this study reveals a gradual shift of dominating sources for PM pollution episodes from SIA to primary sources after starting heating. BaP_{eq} toxicity from coal combustion increased on average by several to dozens of times in the heating period, causing both long-term and short-term health risk. Air mass trajectory analysis highlights the regional influence of the industry emissions from the area south to Beijing. Control measures taken during APEC were found to be effective for reducing industry source, but less effective in reducing the overall $PM_{2.5}$ level. These results provide implications for policy making regarding appropriate air pollution control measures.

1. Introduction

In Beijing, rapid economic development was accompanied by sharp increase of the number of vehicles and air pollution, which poses risk to the public health (Cohen et al., 2017). Particulate matter (PM) is one of the major air pollutants in Beijing. Although a decreasing trend has been observed in recent years due to rigorous mitigation measures, $PM_{2.5}$ level was constantly above the national air quality limit of China (UN Environment, 2019), and haze episodes with high level of $PM_{2.5}$ were often observed and reported (Bei et al., 2020; Yang et al., 2015a, 2020).

Organic matter (OM) is one major component of atmospheric PM, and could constitute 20-90 percent of PM mass (Kanakidou et al., 2005). It accounted for a substantial percentage of Beijng $PM_{2.5}$ during haze as well as non-haze days (Huang et al., 2014; Tian et al., 2016). OM comprises hundreds to thousands of organic species, some of which are particularly source specific and therefore very useful in source apportionment studies of ambient PM pollution. For instance, anhydrosugars (e.g., levoglucosan, mannosan and galactosan) and resin acids (e.g., dehydroabietic acid) are often used as organic markers for biomass burning (Chen et al., 2017; Simoneit et al., 1999). Hopanes are components of mineral oil or coal-based fuels and lubricants (Schnelle-Kreis et al., 2005, 2007). Emitted hopane patterns that represent the distribution and relative level of hopanoid com-

* Corresponding author. State Key Laboratory of Atmospheric Boundary Layer Physics and Atmospheric Chemistry, Institute of Atmospheric Physics, Chinese Academy of Sciences, Beijing, China.
** Corresponding author.
E-mail addresses: xjy@mail.iap.ac.cn (J. Xin); juergen.schnelle@helmholtz-muenchen.de (J. Schnelle-Kreis)
[1] These authors contributed equally to this work as first authors.

https://doi.org/10.1016/j.chemosphere.2021.130143
0045-6535/

pounds/isomers differ substantially with the type and maturity of the (fossil) sources, making them ideal markers for differentiating types of fossil fuel sources, which would be difficult to achieve by other techniques (Saha et al., 2017; Schnelle-Kreis et al., 2005). Poly aromatic hydrocarbons (PAHs) originate from incomplete combustion of fossil fuels (i.e., coal, gasoline and diesel) and biomass (e.g., wood and agricultural biomass) (Chen et al., 2017; Samburova et al., 2013). They are carcinogenic substances (Samburova et al., 2013), and sources that emit a large amount of PAHs may substantially increase the health risk. With the quantification of source specific organic tracers, the ambiguity of source identification can be greatly reduced. However, most chemical characterization studies only measured ions and elements (Huang et al., 2016; Shao et al., 2018; Tan et al., 2016), while organic speciation of $PM_{2.5}$ in Beijing is very limited in comparison with measurements of inorganic chemical components (Ren et al., 2018a, 2019; Yu et al., 2018), and even fewer performed comprehensive chemical characterization with elements, ions and organic tracers (Huang et al., 2014). On the one hand, the conventional solvent extraction and derivatization-based method used for quantifying organic species is time-consuming and labor-intensive. In addition, long-term (i.e. typically 24h) off-line sampling is often necessary for detecting organic trace species (Saha et al., 2017; Yu et al., 2018). The time resolution of such measurement is thus not sufficiently high to track the variation during relatively short pollution episodes (i.e. about 2 to several days). Therefore, a shorter sampling time in combination with a comprehensive chemical characterization including measuring organic species is challenging but desirable for tracing variation of chemical species as well as source contributions. On the other hand, high time-resolved chemical measurement by aerosol mass spectrometry (AMS) techniques provides near real-time mass spectrum profile (m/z ratios after electron ionization) of the sub-micron aerosols, and has been proved advantageous in apportioning PM_1 sources (Elser et al., 2016; Hu et al., 2016; Sun et al., 2012). PMF analyses from AMS measurements, however, are based on complex mass spectra. Single source specific substances can usually not be identified or quantified, which limits the identification of relevant PM sources.

In northern China, there is a major change in emission sources from warm to cold season (Saha et al., 2017; Sun et al., 2015). For instance, in Beijing, domestic heating starts around mid-November. Such changes in source strength could result in increase of air pollution and major change in $PM_{2.5}$ component. During the transition period from autumn to winter in 2014, the APEC summit was held in Beijing during November 10-12, 2014. Several studies focusing on the effectiveness of control measures taken during APEC and the meteorological conditions in improving air quality have been published (Ansari et al., 2019; Liang et al., 2017a; Wang et al., 2016; Xu et al., 2019). Both control measures and favorable meteorological conditions were found to contribute to the reduced $PM_{2.5}$ values during APEC. Unfavorable meteorological condition, e.g., high RH, stagnant air with low surface wind speed, decreased air pressure, and low planetary boundary layer (PBL) height acted as the external driving factors of pollution events (Guo et al., 2014; Wang et al., 2014; Yang et al., 2015b; Zheng et al., 2015). Shortly after the APEC, residential heating in Beijing started officially on November 15, 2014, adding one very important $PM_{2.5}$ source. The chemical composition of $PM_{2.5}$ was reported before and during the APEC; however, these studies covered a limited time period, and a comprehensive investigation on the chemical composition is not available (Ren et al., 2018b; Xu et al., 2019). How the changes of source strengths during the transition period from autumn to winter, the mitigation measures during APEC and the variation of meteorological parameters influenced $PM_{2.5}$ chemical composition, source contributions and toxicity has not been well understood. How these aspects acted individually and interactively is also an interesting topic and is worth studying.

With these questions and research interests, the aims of this study are: 1) Source apportionment of $PM_{2.5}$ by including particulate organic compounds as tracers; 2) Investigation of $PM_{2.5}$ composition and source changes with regard to domestic heating and control measures; 3) Exploration of the effects of source strength and meteorological changes on $PM_{2.5}$ level and its chemical compositions; 4) Evaluation of the PAH associated health risk and its source contributions.

To meet these aims, this study particularly applied a partially high time resolution (every 6h) off-line sampling in combination with a very sensitive in-situ derivatization thermal desorption gas chromatography mass spectrometry method (IDTD-GC-TOF-MS) previously developed by the author's lab (Li et al., 2018a, 2018b; Orasche et al., 2011). The high analytical sensitivity of this method meets the requirement for detecting and quantifying trace organic species sampled in short time period.

2. Material and methods

2.1. Sampling, $PM_{2.5}$, gaseous pollutants and meteorology

Ambient $PM_{2.5}$ was sampled on the roof of a 2-story building on the premises of the Institute of Atmospheric Physics, Chinese Academy of Sciences between the north ring-3 and ring-4 of Beijing (39.9744 N, 116.3720E). It is a typical urban site in Beijing. Quartz fiber filters (Pall Life Sciences, Ann Arbor, MI, USA; d = 150 mm) were prebaked before sampling to avoid any interference with organic matter analysis. Samples were taken from October 24th to December 7th, 2014 using $PM_{2.5}$ samplers (Digitel DHA-80, Switzerland) with an airflow rate of 0.5 m^3 min^{-1}. Blank filters were used for quality control. A total of 68 samples with 6h sampling time (0:00-6:00, 6:00-12:00, 12:00-18:00, 18:00-24:00) and 26 samples with 24h sampling time (0:00-24:00) were used in chemical and statistical analyses. Most of the 6h samples were taken during $PM_{2.5}$ pollution episodes. Meteorological data was obtained from the China Meteorological Administration. $PM_{2.5}$ mass concentrations were measured by a tapered element oscillating microbalance (TEOM 1405-DF, Thermo Scientific, USA) and gaseous species (SO_2, O_3, NO_X, and CO) were measured by commercial instrument (Model series I, Thermo Scientific, USA).

2.2. Chemical analysis of ions and elements

NH_4^+ was analyzed by a continuous flow analyzer (CFA) (Scan + +, Skalar, The Netherlands), and anions (NO_3^-, SO_4^{2-} and Cl^-) were analyzed by ion chromatography (ICS-1500, Dionex, USA). Punched filter samples with a diameter of 25 mm were extracted three times in 5 ml de-ionized water (Milli-Q, 18.2 MΩ cm), each in ultrasonic bath for 15 min and filtered.

Elements were measured by inductively coupled plasma atomic emission spectroscopy (Optima 7300 DV, PerkinElmer, Germany) following sample digestion. The measured spectral element lines (nm) for each element are: Al (167.078), As (189.042), B (249.773), Ba (455.404), Ca (183.801), Cd (214.438), Co (228.616), Cr (267.716), Fe (259.941), K (766.491), Li (670.780), Mg (279.079), Mn (257.611), Mo (202.030), Na (589.592), Ni (231.604), P (177.495), Pb (220.353), S (182.034), Se (196.090), Sn (189.991), Sr (407.771), Ti (334.941), V (292.464), and Zn (213.856).

2.3. Chemical analysis of organic species

In-situ Derivatization Thermal Desorption Gas Chromatography Time-of-Flight Mass Spectrometry was applied to measure the concentrations of organic species in $PM_{2.5}$. Orasche et al. (2011) described the details of this method. It can simultaneously measure polar and nonpolar species in one analytical run. In this study, only primary species were quantified/semi-quantified before secondary markers were

integrated in this method (Li et al., 2018a, 2018b). The species discussed in this manuscript include 14 PAHs, 17 alkanes from C21 to C36, 10 hopanoid compounds, and 4 biomass burning markers (see Fig. 3 and Table S1 for the PAHs, hopanes and anhydrosugars in detail).

2.4. PMF

Source apportionment analysis was conducted using the EPA PMF 5.0. It has become the most popular receptor model applied for PM source apportionment studies in China (Zhu et al., 2018). One advantage of PMF is that it does not require profiling in advance although prior knowledge on source profiles is helpful for factor interpretation. In principal, PMF works better with a large number of independent samples that far exceed the number of variables (Pant and Harrison, 2012). In this study, 94 observations were available for analysis. A sample-to-variable ratio of 3:1 was suggested as the minimum to get an accurate result (Pant and Harrison, 2012; Thurston and Spengler, 1985), and therefore only a subset of the measured species were included in PMF, including benz[a]anthracene, chrysene, sum_benzofluoranthenes (benzo[b]fluoranthene, benzo[j]fluoranthene and benzo[k]fluoranthene were quantified together as sum_benzofluoranthenes because of co-elution), benz[e]pyrene, benz[a]pyrene, dibenz[ah]anthracene, indeno[1,2,3-cd]pyrene, picene, benzo[ghi]perylene, coronene, retene, 31abS, 31abR, dehydroabietic acid, mannosan, galactosan and levoglucosan, chloride, nitrate, sulfate, ammonia, Al, As, Ca, Cd, K, Mg, Na and Pb. The majority of PAHs was included in order to calculate the PAHs based toxicity of each source factor. $PM_{2.5}$ mass concentration was set as the total variable. The Fpeak result of PMF analysis will be presented in the results and discussion part as it is more robust in bootstrap analysis. The verification of 6 factor solution and the Fpeak result is presented in supplementary material.

2.5. Calculations of BaP_{eq} toxicity

Toxicity equivalency factor (TEF) values proposed by Nisbet and LaGoy (1992) are often used to calculate the toxicity of PAHs mixtures. Based on this approach, all carcinogenic PAHs were given specific TEFs between 1 and 0 relative to the toxicity of benzo[a]pyrene as the reference compound. The BaP_{eq} (benzo[a]pyrene equal concentration) of each sample was calculated by summing up the BaP_{eq} of each individual PAH, namely the individual PAH concentration multiplying its TEF. BaP_{eq} for each source could be calculated in the same way. Then the PAHs related potential toxicity contribution of each source was calculated by multiplying source contribution and the BaP_{eq} of that source, which was further scaled to the BaP_{eq} of each sample to yield the BaP_{eq} toxicity contribution of a specific source to that sample.

2.6. Back trajectory analysis

To assess the influence of transported PM and to identify potential source regions, particularly for air pollution episodes, back trajectory analysis was done using the HYSPLIT-4 (HYbrid Single-Particle Lagrangian Integrated Trajectory) model developed by NOAA/ARL (U.S. National Oceanic and Air Administration/Air Resources Laboratory). The 48h trajectories ending at the height of 200 m above ground level were calculated each 6 h during the sampling period, terminating at the 3, 9, 15 and 21 O'clock of local time.

3. Results and discussions

3.1. Characterization of pollution episodes, heating and APEC periods with regard to chemical composition and meteorological conditions

In this study, a pollution episode is defined as a period when the 6h or 24h $PM_{2.5}$ concentration was above the threshold level of 125 μg m^{-3} and lasted for at least 36h (for 6h samples) or 2 days (for daily samples). Five episodes (EP1 - EP5) were identified during the sampling period (Table 1). APEC period was from the 3rd to 12th of November. The non-episode (non-EP) referred to all the remaining time periods other than episodes and APEC. The study period was also divided into pre-heating and heating periods by the day when official heating started (the 15th of November).

3.1.1. General chemical and meteorological characterization of episodes, heating period and APEC period

The episodes (EP1-EP5) were generally associated with high RH, low pressure and low wind speed (WS) as shown in Fig. 1, Table S1 (Supplementary material) and Fig. S1. From chemical perspective, episodes were associated with a global increase in concentrations of PM mass, NO_2, SO_2, CO, secondary inorganic ions, most elements (i.e., As, Cd, Pb, Co, Cr, Mn, Li, Mo, Na, Ni, P, Se, Sn and Zn), and levoglucosan, but a decrease in O_3 concentration. PM mass concentrations showed high correlation with CO, NO_2 and SO_2 (Fig. 1, Fig. S2, and Fig. S3) but with exceptions. Some crustal elements (i.e., Al, Ca, Mg, Sr and Ti) showed limited variations in concentration. Three types of organic species, PAHs, alkanes and hopanes, generally were at low levels in pre-heating period. In contrast to pollution episodes, meteorological conditions, PM level and gaseous pollutants during APEC were on a comparable level with non-episodic days before the heating period. Back trajectories for defined periods are shown in Fig. 2. The air masses during the episodes mostly came from the area south to Beijing, whereas air masses during the APEC and the non-episode originated predominately from the northwest and traveled long distance. Actually, an approximate synchronization between the change of trajectories and the start and end of an episode could be observed. Specifically, at the beginning of a haze episode, PM started to increase or accumulate when the trajectory changed from northwest (west China or Mongolia) to south (Beijing (south)-Tianjin-Hebei: BTH regions), and the episodes ended when the trajectories changed to northwest.

3.1.2. Variations of secondary inorganic ions and primary organic species after heating started

As the most abundant measured chemical species, secondary inorganic ions contributed a lot to PM masses. After the start of domestic heating, several changes of concentrations or patterns of secondary inorganic ions could be identified. Firstly, nitrate and ammonia concentrations were much higher during episodes in the pre-heating period than in those in the heating period. Moreover, nitrate/sulfate ratio was

Table 1
Time period for each episode and APEC. EP1 to EP5: episode 1 to episode 5.

	EP1	EP2	EP3	EP4	EP5	APEC
Start time	24.10.2014	30.10 0:00-5:00	19.11 0:00-12:00	25.11 6:00-12:00	28.11 18:00-24:00	3.11
End time	25.10.2014	01.11 0:00-6:00	21.11 6:00-12:00	27.11 0:00-6:00	30.11 0:00-6:00	12.11
Duration	2 days	2 days	2.5 days	1.75 days	1.5 days	10 days

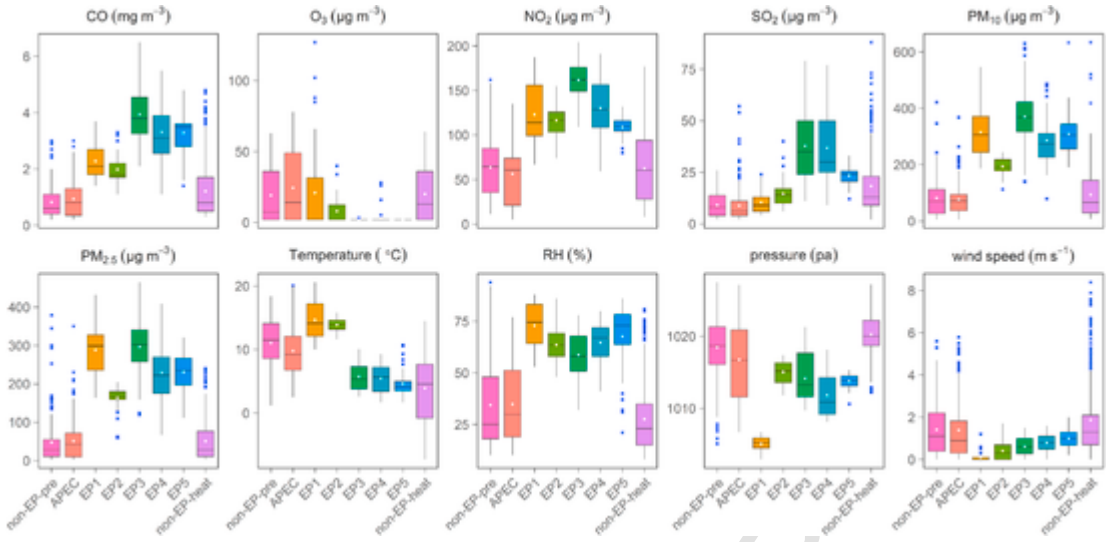

Fig. 1. Box plots of $PM_{2.5}$, PM_{10}, gaseous pollutants (O_3, CO, SO_2, and NO_2) and meteorological parameters (temperature, pressure, RH and wind speed) during APEC, pollution episodes and non-episode in autumn-winter 2014. EP1 to EP5: episode 1 to episode 5, non-EP-pre: non-episode time during pre-heating period and non-EP-heat: non-episode time during heating period. White dot and the line in the middle of the box represent the mean and median, respectively.

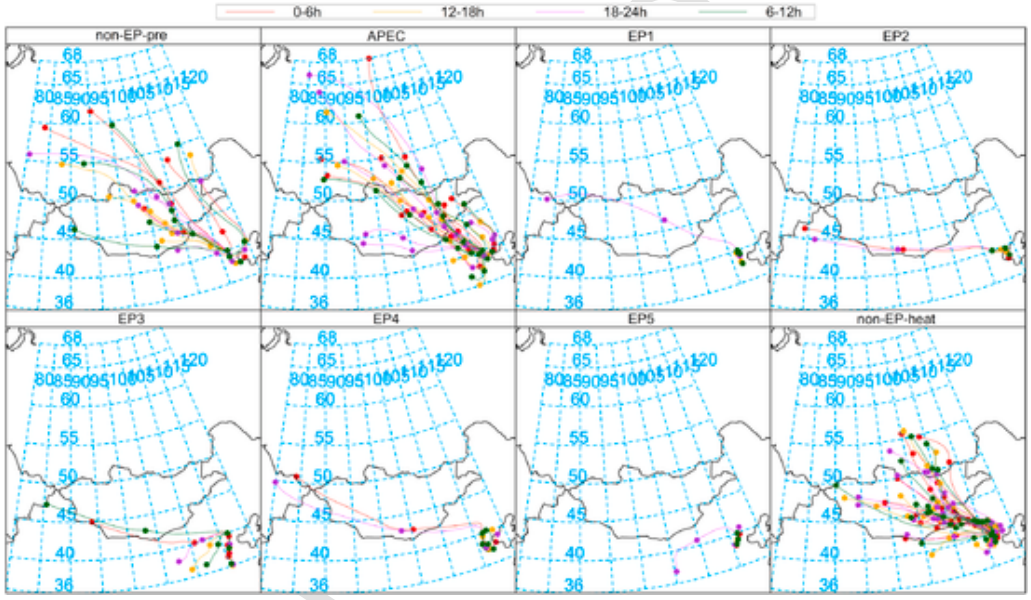

Fig. 2. 48-h backward trajectories arrived at Beijing (at 200 m AGL) during APEC, pollution episodes and non-episode in autumn-winter 2014. EP1 to EP5: episode 1 to episode 5, non-EP-pre: non-episode time during pre-heating period and non-EP-heat: non-episode time during heating period.

also much higher in pre-heating period (1.9-2.4 on average) than in heating period (1.0-1.6 on average), although sulfate is significantly correlated with nitrate (Fig. S3, r = 0.93, $P < 0.01$). To study the formation of nitrate and sulfate, the nitrogen oxidation ratio (NOR = $n\text{-}NO_3^-/(n\text{-}NO_3^- + n\text{-}NO_2)$) and sulfur oxidation ratio (SOR = $n\text{-}SO_4^{2-}/(n\text{-}SO_4^{2-} + n\text{-}SO_2)$) are often calculated for the characterization of NO_2 and SO_2 oxidation degree, respectively. Calculated SOR and NOR in this study indicate higher degree of oxidation (higher SOR and NOR values) for SO_2 and NO_2 during episodes than in non-episode periods as expected, and higher during pre-heating episodes than heating episodes (Table S1). Regarding SIA, high RH is considered very important for heterogeneous and aqueous phase formation pathways, which is believed to be responsible for rapid formation of SIA during pollution episodes when gas-phase reaction were often reduced due to decreased gaseous oxidants (i.e. O_3) (Tan et al., 2018; Zhao et al., 2013; Zheng et al., 2015). As shown in Fig. 4A and Fig. 4B, starting from RH at about 20%, SOR and NOR increased substantially with the increase of RH during pre-heating period. Interestingly, the effect of RH on SOR or NOR was found to be much weaker during the heating period. A positive yet similar correlation was found between NOR and SOR both in pre-heating and heating periods (Fig. 4C and Fig. S3, r = 0.73, $p < 0.01$). On the other hand, temperature and atmospheric oxidants play an important role in the oxidation reactions to form secondary aerosols, namely SIA and secondary organic aerosol (SOA) (Huang et al., 2016; Li et al., 2020). From Fig. 4, it can be seen that the temperature was substantially different between pre-heating period and heating period. The SOR and NOR values were also related to temperature (Fig. 4D and E).

Primary organic species PAHs, hopanes and alkanes showed very high positive correlation within each compound class and between compound classes (most r > 0.9, $p < 0.001$). Their concentrations were much higher (several to dozens of times increase on average) dur-

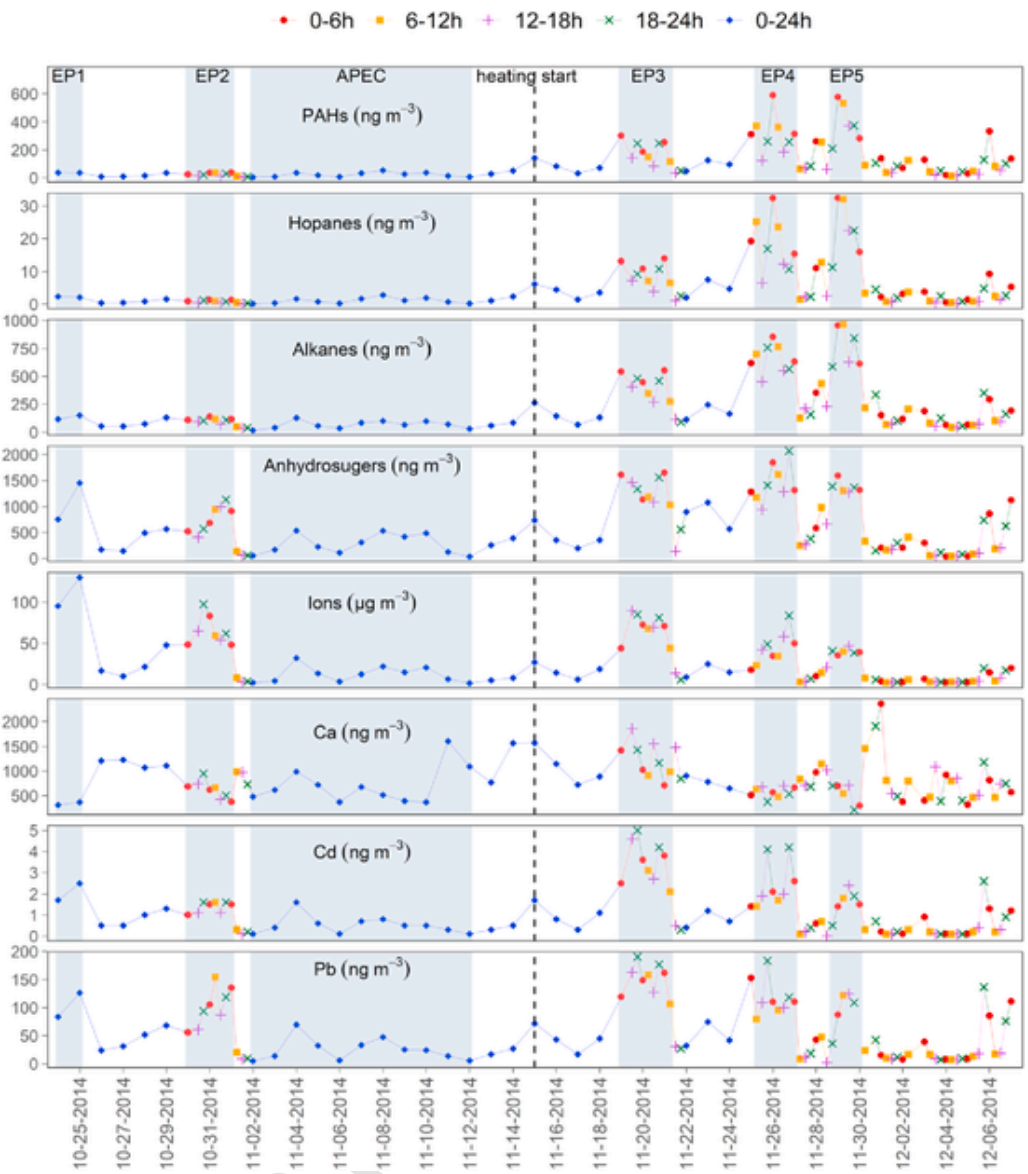

Fig. 3. Temporal variations of the characteristic chemical species in $PM_{2.5}$ in Beijing. PAHs include fluoranthene, pyrene, benz[a]anthracene, chrysene, sum_benzofluoranthenes, benz[e]pyrene, benz[a]pyrene, perylene, dibenz[ah]anthracene, indeno[1,2,3-cd]pyrene, picene, benzo[ghi]perylene, coronene, and retene. Hopanes include 18a(H)-22,29,30-trisnor-neohopane (Ts); 17a(H)-22,29,30-trisnorhopane (Tm); 17a(H),21b(H)-30-norhopane(29ab); 17b(H),21a(H)-30-norhopane (29ba); 17a(H),21b(H)-hopane (30ab); 17b(H),21a(H)-hopane (30ba); 17a(H),21b(H)–22S-homohopane (31abS); 17a(H),21b(H)-22R-homohopane (31abR); 17a(H),21b(H)–22S-bishomohopane (32abS); 17a(H),21b(H)-22R-bishomohopane (32abR). Alkanes include C21 to C31. Anhydrosugars include levoglucosan, mannosan and galactosan. Ions include sulfate, nitrate, ammonium and chloride.

ing heating episodes than pre-heating period (Fig. S2 and Table S1). Particularly, they were also at high level during the relatively "clean" (non-EP-heat) days in heating period. In addition, distinct differences in general organic patterns and differences in the ratios between individual PAHs or hopanes were observed during the sampling period as shown in Fig. 5.

As very unique and useful source identification indicators, three source indicative diagnostic ratios of hopanes were calculated, namely the 30ab/29ab ratio, the homohopane index (31abs/(31abS + 31abR)) and the hopane/moretane ratio of 30ab/30ba. Firstly, 29ab was dominant over 30ab during heating period and the opposite was observed in the pre-heating period. Secondly, the average homohopane index decreased from 0.55 during pre-heating period to 0.44 during heating period. Similar decrease was also observed for the bishomohopanes (32abs/(32abS + 32abR)) in this study. Thirdly, the hopan/moretane ratio (30ab/30ba) and the ratio of 29ab/29ba were much lower during heating period comparing to pre-heating period.

Regarding PAH pattern, higher percentage of relatively volatile fluoranthene, pyrene, chrysene, benzo[a]anthrazene and retene was observed in the heating period, especially after the end of November (Fig. 5B) when the temperature decreased dramatically (Fig. S1). Benzo[a]pyrene was slightly higher than benzo[e]pyrene during the heating period while the opposite was observed during the pre-heating period (Fig. 5D). Alkanes also demonstrated slightly different pattern from pre-heating to heating periods. During the pre-heating period, C29 and C31 had higher percentages (Fig. S4) (Ren et al., 2018a), whereas in the heating period, C22 - C25 were found to be the dominating alkanes. Similar to PAHs, an increase of percentages of lighter alkanes could be observed for the heating period, particularly after substantial decrease of temperature (Fig. S4). The biomass burning markers (i.e. anhydrosugers) increased slightly during the heating episodes comparing to other episodes (Fig. S2) and non-episode, but the increment was much less prominent compared with the PAHs, alkanes and hopanes.

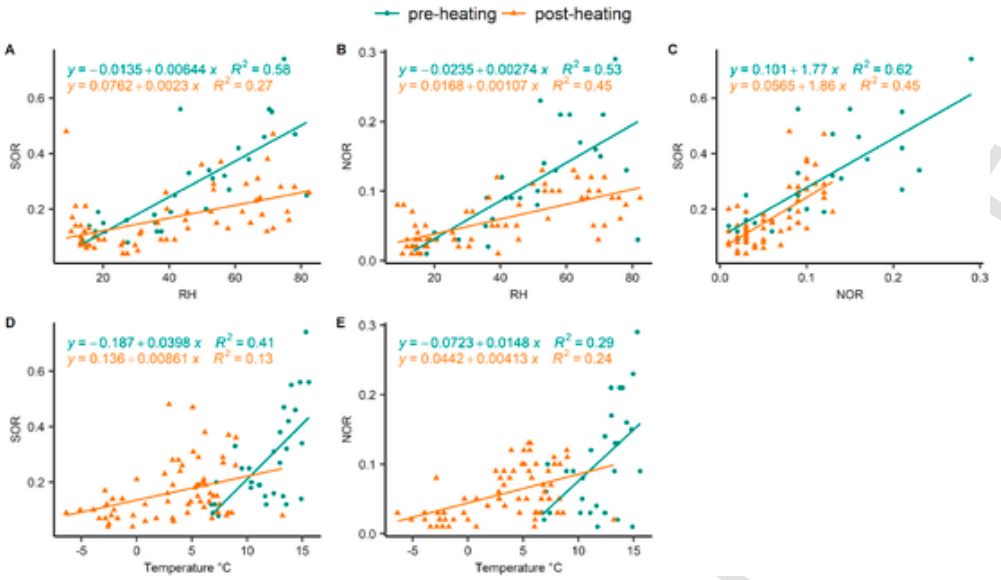

Fig. 4. The relationships between SOR and RH (A), NOR and RH (B), SOR and NOR (C), SOR and Temperature (D), and NOR and Temperature (E) in the pre-heating (before 15th November) and heating periods (after 15th November).

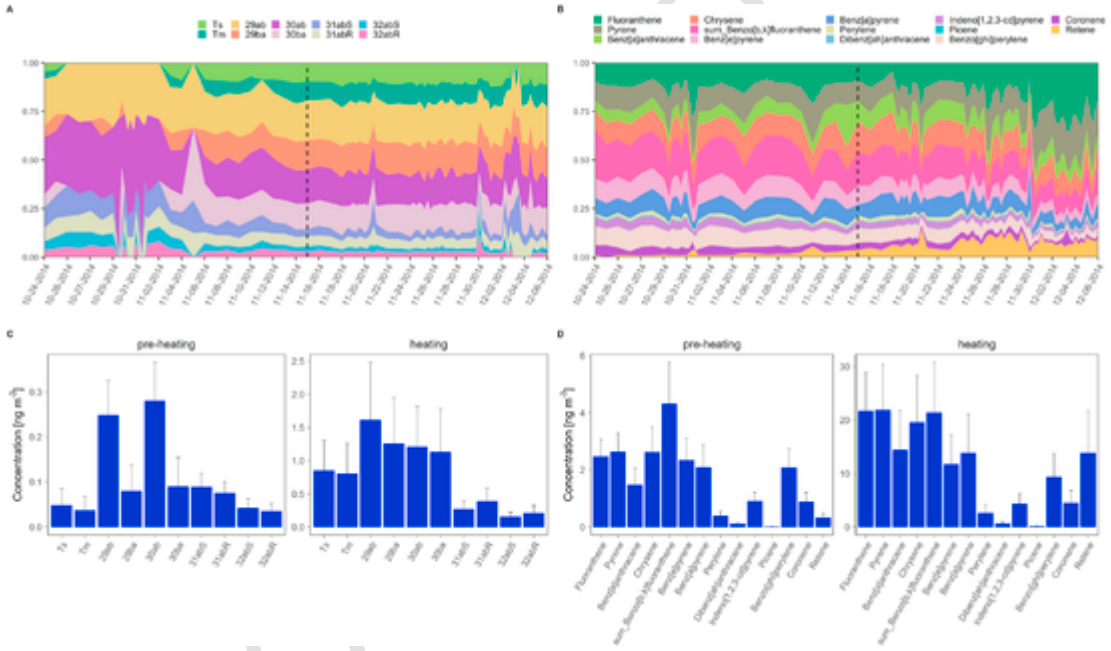

Fig. 5. The temporal variations of the contributions of individual hopane to sum of hopane (A), and individual PAHs to sum of PAHs (B); and the pattern of organic species for hopane (C) and PAHs (D) in Beijing in autumn-winter 2014.

3.1.3. Summary of observatory results

Many studies have explored the effect of meteorological change on pollution episode formation in Beijing. Results from previous studies have related high PM concentrations in Beijing to southern trajectories and stagnant meteorological conditions (Sun et al., 2006; Zhang et al., 2013), which is in line with the result of this study. Zheng et al. (2015) found that vanishing of winter haze episodes in Beijing was always accompanied by the Siberian anticyclone, in consistent with the rough synchronization of air mass change with the haze start/stop observed in this study. Although the changes of air mass trajectories and meteorological conditions were closely related to the haze formation/vanishing, the reason behind the variations of the aerosol levels lies in the concentration changes of thousands of chemical species, which come from primary and secondary sources, and can be traced back to anthropogenic and biogenic emissions. Meteorological conditions indeed played an important role in air pollution in Beijing, but the $PM_{2.5}$ sources are the underlying reason. Therefore, identifying the significant sources and reducing respective source contributions may be the ultimate solution of air pollution.

From the variation of measured chemical species, strong indication of changes in the strength of sources contributing to Beijing $PM_{2.5}$ and pollution episodes could be seen. Particularly, obvious change occurred after heating started. Firstly, the high nitrate/sulfate ratio for pre-heating time is in line with the study by Gao et al. (2015), who found higher nitrate/sulfate ratio in autumn than in winter. Even lower nitrate/sulfate ratio (0.68 ± 0.44) was reported during the haze episode in January, 2013 (Han et al., 2016). This trend indicates a relative

decrease in mobile source (NO_x source) contribution in comparison with stationary combustion source (SO_2 source) contribution to $PM_{2.5}$ from pre-heating to heating period (Gao et al., 2015; Han et al., 2016). SIA was often identified as the main contributor to particulate matter pollution in Beijing under unfavorable meteorological condition as also observed in this study; and its formation was often related to high RH (Han et al., 2016; Liu et al., 2018; Zhao et al., 2013). Under high RH, hygroscopic growth of sulfate and nitrate can absorb water continuously to increase the liquid water content in the aerosols (Yang et al., 2015b). Aqueous phase formed on the surface of droplet mode aerosol greatly increases the aqueous phase and heterogonous reaction of gaseous pollutants. This is probably the reason for the strong positive effect of RH on SOR and NOR levels during pre-heating episodes. Despite this positive correlation of RH with SIA, they are obviously not the cause of decreased oxidation degree of NO_2 and SO_2 from pre-heating to heating period. The low temperature during heating period (Fig. 4D and E) and extremely low concentration of ozone (as gaseous oxidant) could result in low oxidation rate. However, none of them could fully explain the oxidation of NO_2 and SO_2. Whether the much higher concentrations of waster insoluble primary organic species (i.e., non-polar organic compounds) measured during heating period contribute to the decreasing of the positive feedback of hygroscopic growth of sulfate and nitrate during the heating period needs further investigation. In summary, the formation of SIA is complex and dependent on interactions of multiple parameters.

Hopane diagnostic ratios are very useful and specific source indicators. The IDTD-GC-MS method helped having the trace amount of low abundance hopanoid isomers quantified to calculate the ratio. According to the study of Zhang et al. (2008), 29 ab is mainly emitted by Chinese coal burning except industrial bituminite, while 30 ab is mainly from vehicle exhaust. A predominance of 29 ab during heating period is therefore an indication of coal combustion contribution. The decrease of homohopane index observed during heating period is in line with the homohopane index trend from about 0.6 in summer to 0.5 in winter as reported by Wang et al. (2009). From the study of Schnelle-Kreis et al. (2005), the homopopane index is higher in mineral oil-derived emission sources (about 0.6) than in coal combustion (0.1–0.35). In summary, the changes of hopane diagnostic ratios indicated a shift of predominating hopane origin from mineral oils (i.e., vehicle exhaust) in pre-heating period to solid fuel (i.e., coal combustion) in heating period. Particularly, as the most indicative ratio to discriminate the sources, the homohopane index played a key role in the interpretation of PMF analysis results to assign source factors to coal combustion and traffic emissions as will be discussed in following text. In addition to hopane diagnostic ratio changes, the change of predominating alkanes from C29 and C31 in pre-heating period to C22 - C25 in heating period is also an indication of shift of dominating source from biologic emission (Schnelle-Kreis et al., 2005) to Chinese coal combustion emission (Zhang et al., 2008). The pattern change of PAH and alkanes were not so characteristic as for Hopanes, the lower percentage of relatively volatile PAHs and Alkanes may be partly explained by the increased partition to the particle phase at lower temperatures. Unlike Hopanes and PAHs, the biomass burning markers does not show heating-related trends. This could result from additional contribution of agricultural biomass burning in autumn in the pre-heating period (Chen et al., 2017; Zhang et al., 2013).

3.2. PMF source apportionment

3.2.1. Source characterization

PMF analysis successfully resolved 6 sources in this study, which are assigned as the secondary inorganic aerosol (SIA), coal combustion (Coal), traffic emissions (Traffic), biomass burning (BB), dust, and industry emissions (Industry) based on the resolved source profile (Fig. 6). On average, they accounted for 45, 12, 12, 7, 2, and 23 μg m^{-3} of the average $PM_{2.5}$ concentration, respectively. The only secondary source resolved in this study is the SIA, while the rest 5 sources are of primary origin. Fig. 7 demonstrates the time series based variation and average diurnal variation of source contributions.

SIA source was dominated by nitrate, sulfate and ammonia. SIA was often the lowest in the morning during 6:00-12:00, accompanied by the lowest SO_2, NO_2, SOR, NOR levels and nitrate/sulfate ratio. SIA mostly reached high level during 12:00–18:00, or during 18:00-24:00, associated with the highest NO_2, SOR, and NOR levels, which is in line with the result of hourly secondary ion concentrations in January 2013 from Han et al. (2016).

Coal combustion source was identified by a homohopane index of 0.35. Coal combustion was also a dominating contributor to PAHs, which is in line with previous studies (Saha et al., 2017; Zhang et al., 2008). Coal combustion source contribution often reached high levels during 0:00-6:00, and was the lowest during 12:00-18:00. Both the meteorological conditions (i.e., low temperature and low PBL) and elevated source activities resulted in large contribution of coal combustion during night, while the higher PBL and lower emissions in the afternoon led to lower source contribution.

Traffic emission source factor was identified by a homohopane index of 0.48, which was much larger than the index from the coal combustion source (0.35). It explained a small fraction of PAHs and heavy metals such as As, Cd and Pb. Its diurnal variability was not as obvious as the other two primary emissions of coal combustion and BB as will be discussed below. Traffic emission was on average lowest during 12:00-18:00. During episodes, its maximum level occurred during different time periods.

The industry source factor was characterized by Cl^- and heavy metals such as As, Cd and Pb. Source study of elements and ion in Beijing has identified industry as a main source for Cd and Cl^- (Han et al., 2007). The industry source contribution was highest during 18:00-24:00 and low during 0:00-6:00 or 6:00-12:00. This might be related to both the south activity and the transport delay of industry emission to the sampling site as air mass transportation seems to play an important role in high industry contribution, which will be discussed below.

Biomass burning source was recognized by high load of organic markers of dehydroabietic acid, mannosan, galactosan and levoglucosan. Their diurnal variation was similar to coal combustion with the peak value occurring mostly during 0:00-6:00 and the lowest level was found during 12:00-18:00, indicating its domestic heating origin.

Dust source was characterized by crustal-related elements of Al, Ca and Mg (Zhang et al., 2013). Dust was the only source with comparable contribution to $PM_{2.5}$ concentration between episodes and non-episode while all anthropogenic sources showed higher contributions during episodes. It showed very weak diurnal variation with slightly higher contribution during 12:00-18:00 and lower contribution during 0:00-6:00.

3.2.2. Source contributions between pre-heating and heating periods, and among pollution episodes

The source contribution to $PM_{2.5}$ for each episode was calculated and the average contribution of each source during every defined period as well as the residue (the difference between measured $PM_{2.5}$ concentration and the PMF source predicted $PM_{2.5}$ concentration) are shown in Fig. 8. Generally, the major sources included SIA, traffic emission, coal combustion and industry, while BB and dust contributed a small part to $PM_{2.5}$. The main sources of $PM_{2.5}$ varied among each period. In the pollution episodes, there were 1-4 dominating sources of $PM_{2.5}$, while in non-episode period the source contributions were more evenly distributed.

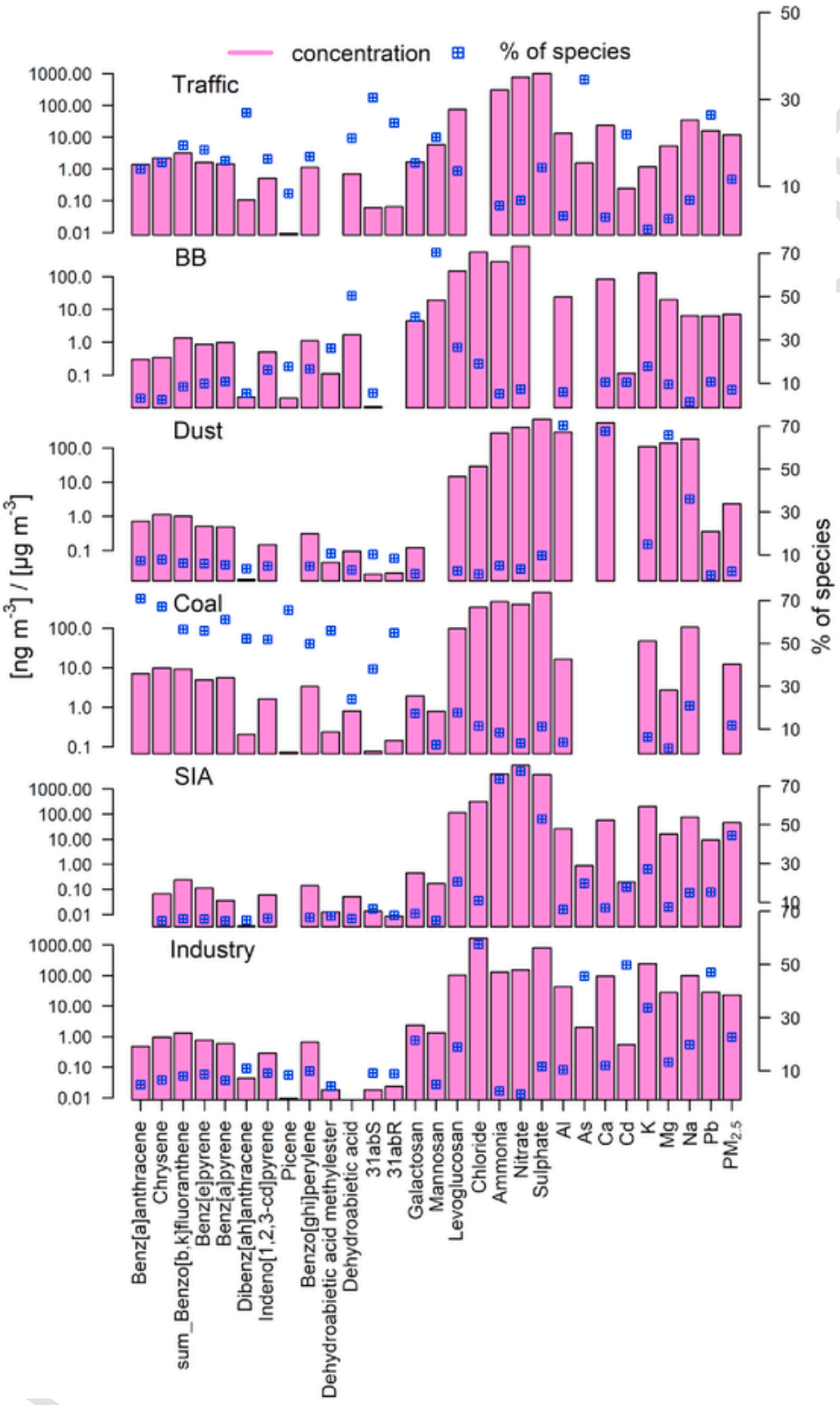

Fig. 6. The $PM_{2.5}$ source profiles of Traffic, BB (biomass burning), Dust, Coal (coal combustion), SIA (secondary inorganic aerosol), and Industry (industry emission).

The episodes show distinctions in source contributions, resulting in different "types" of $PM_{2.5}$ episodes. One significant result from this chemical marker-based source apportionment study is the prominent change in source contribution related to heating activity as indicated by the variations of chemical profile mentioned above. A significant increase of primary coal combustion and meanwhile a remarkable decrease of SIA from pre-heating period to heating period were observed (Fig. 8). This is the case both for episodes (EP1 and EP2 in comparison with EP3 - EP5) and non-episodes (non-EP-pre and APEC in comparison with non-EP-heat). Contribution from SIA was particularly high during pre-heating pollution episodes, making SIA the only major dominating aerosol source for these two episodes (contributing 282.9 ± 105.2 µg m^{-3} and 152.1 ± 34.9 µg m^{-3}, respectively). Contribution from SIA among non-EP-pre days was significantly lower (20.1 ± 28.8 µg m^{-3}),

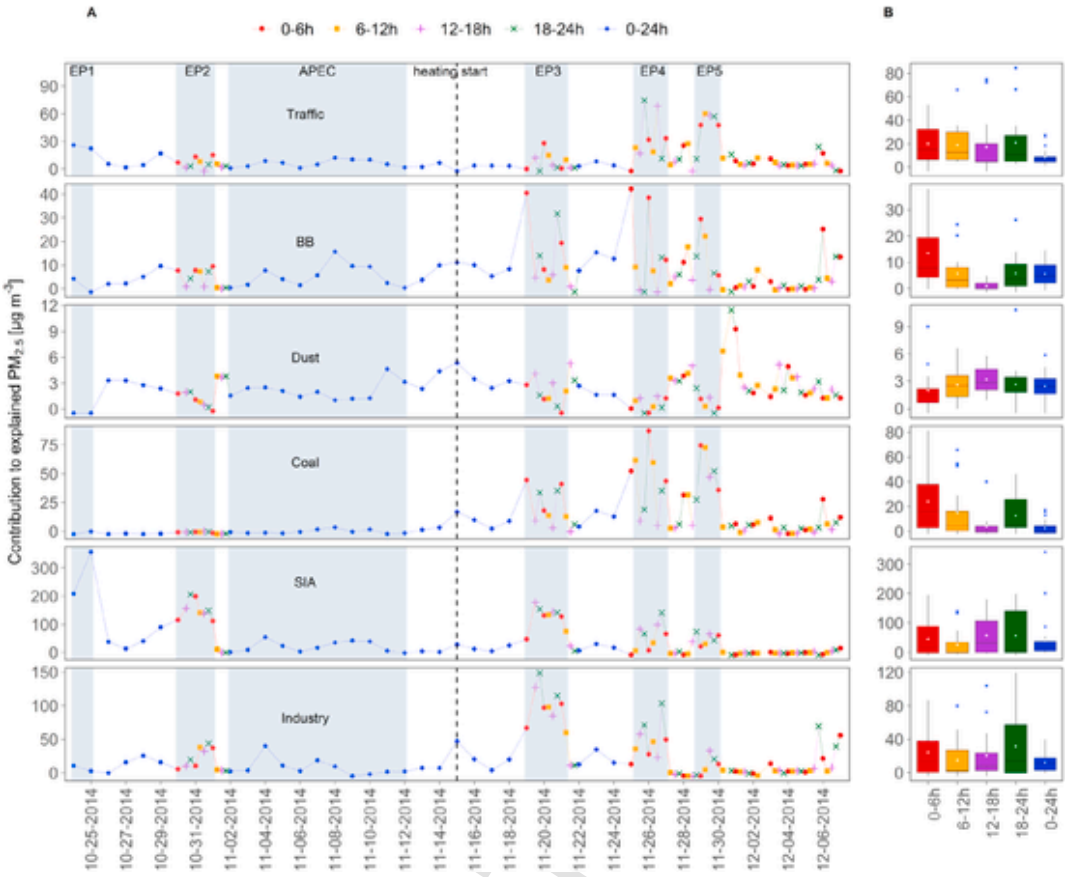

Fig. 7. Time series of the source contributions (A) and boxplot of the diuranl variaton (B).

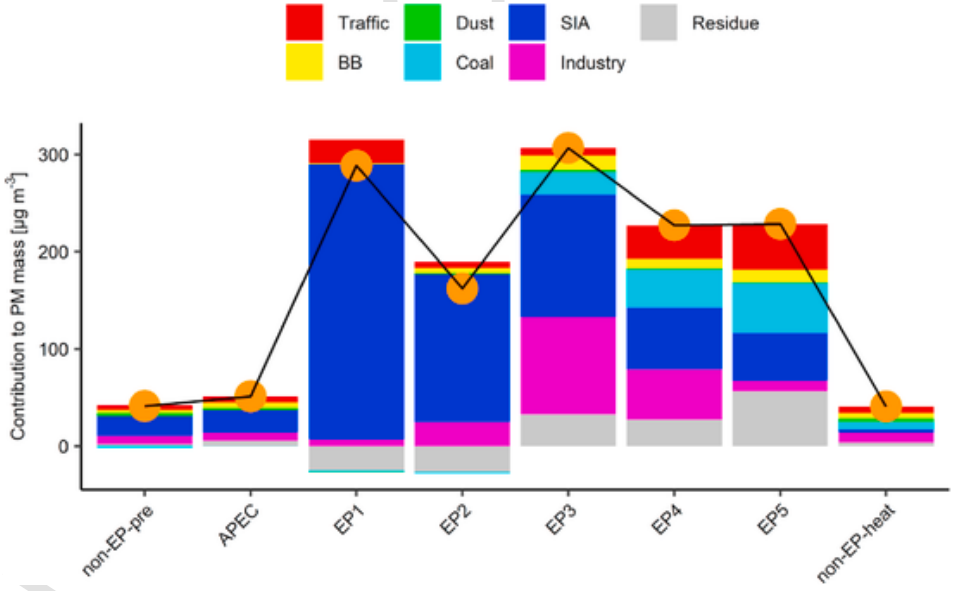

Fig. 8. The average contributions of different sources to $PM_{2.5}$ mass concentration (average value indicated by orange dots) in pollution episodes, APEC and non-episode. EP1 to EP5: episode 1 to episode 5, non-EP-pre: non-episode time during pre-heating period and non-EP-heat: non-episode time during heating period. BB: biomass burning; SIA: secondary inorganic aerosol. (For interpretation of the references to colour in this figure legend, the reader is referred to the Web version of this article.)

but still several times higher than during non-EP-heat days (3.4 ± 11.7 μg m^{-3}). It is worth mentioning that the modelled residue for EP1 and EP2 were negative, meaning that more $PM_{2.5}$ was modelled than actual level, indicating higher modelled SIA contribution than actual contribution. The reason for this would be discussed in the following section. Whereas, coal combustion had negligible contribution during pre-heating period compared to gradually increasing contribution to a significant level during heating period (EP3 - EP5: 23.4 ± 15.2 μg m^{-3}, 40 ± 28.6 μg $m^{-3}$and 51.6 ± 19.1 μg m^{-3}, respectively; and non-EP-heat: 7.7 ± 10.9 μg m^{-3}).

Another two primary sources demonstrating interesting variation are traffic and industry emissions. During non-episodes, their contribu-

tions are comparable between pre-heating periods and heating-period, with slightly higher contribution during heating period. However, among episodes, traffic emission was high during EP5 (47 ± 18.6 μg m^{-3}) and EP4 (34.8 ± 24 μg m^{-3}), while much lower during EP2 (6.3 ± 5.9 μg m^{-3}) and EP3 (7.7 ± 9.7 μg m^{-3}). Industry source contributed more to $PM_{2.5}$ during EP3 (100 ± 28.1 μg m^{-3}) and EP4 (51.9 ± 26.2 μg m^{-3}) than during EP1 (6.8 ± 5.6 μg m^{-3}) and EP5 (10.7 ± 14.7 μg m^{-3}).

3.2.3. Effect of source strength and meteorological conditions on source contributions

Although the meteorological change could be the external cause of pollution episode, the strength of PM sources is the essential reason of air pollution. Therefore, both their influence should be reflected in the variations of air pollution and source contributions. In this study, the source strength of primary coal emissions is clearly seen from the semi-quantitative source apportionment result, causing a much higher coal source contribution in the heating period regardless of the meteorological condition. But the pollution episode of the heating period is still related to the meteorological parameters, particularly air mass trajectories. Industry emission was also one important primary source, which contributed on average 14.6% ± 12.8% during 2010-2016 to Beijing $PM_{2.5}$ (Yang et al., 2015c; Zhu et al., 2018). Combined influence of air mass trajectories and source strength on contribution of industry source could be seen in the much higher industry contribution found in EP3 and EP4. As shown in Fig. 2, the trajectory of EP3 is from southwest, where a lot of industries are located (Qi et al., 2017; Yang et al., 2015c). Similar situation occurred in EP4. Except during these two episodes, industry was not the main source for Beijing $PM_{2.5}$. In this study, industry sources are mainly recognized by toxic heavy metals. Therefore, the relatively stable harmful pollutants can be transported from surrounding areas to cities, causing health risk. Simply relocating heavily polluted industries to rural sites could not completely eliminate air pollution and potential health risk. Traffic as another main primary source was found to contribute averagely 14.5% ± 8.9% to Beijing $PM_{2.5}$ during 2010-2016 (Zhu et al., 2018), and it made the highest contribution to $PM_{2.5}$ during EP5 in this study (Fig. 8). The more localized and circulated air mass trajectories around the south of Beijing during EP5 indicated the high level of source contribution from Beijing local traffic emission. The direct contribution of traffic emission in this study was prominent under low temperature when primary emission sources dominated the PM pollution as in EP5. Under higher temperature during pre-heating period when secondary aerosol dominated, high nitrate to sulfate ratio demonstrated the dominating of secondary ions from traffic emission (NOx) over industry emissions (SO_2), highlighting the contribution of primary traffic emission as precursors of secondary ions. It is consistent with the relatively high contribution of motor vehicles as the primary source (Yang et al., 2015b). For primary sources, the influence of source strength and meteorological conditions are generally directly reflected. However, for the SIA, the combined effect is relatively indirect and more complex. Both the abundance of primary precursors and the oxidation degree play important role. During EP1 and EP2, a stagnant meteorological condition with low pressure, low wind speed and low PBL was observed (Fig. 1), which would result in a substantial decrease of the dispersion of gaseous and particle phase pollutants. Meanwhile, the relatively high RH, temperature and O_3 facilitated the gas phase and particulate phase chemical oxidation reactions, leading to formation of SIA. A positive feedback could be expected under such condition since fast aqueous phase reaction occurred also on freshly formed and accumulated particulate matter phase (Sun et al., 2006; Zhang et al., 2018). It is worth mentioning that such condition could also facilitate the formation of SOA. Although SOA was not resolved in this study due to lack of measurement of appropriate markers, its contribution might have been partially reflected in the very high SIA contribution resolved in EP1 and EP2 during pre-heating period. During heating episodes, the positive residue not modelled by the resolved sources may be partially attributed to SOA (Fig. 8). However, similar stagnant condition (i.e. low pressure, low wind speed) and high RH during heating episodes, particularly EP4 and EP5, did not lead to high SIA level. On the one hand, the low temperature and O_3 concentration during heating episodes could have resulted in decreased chemical formation reactions. On the other hand, further studies are needed to investigate if the measured high abundance of non-polar organic species had modified the chemical property of the aqueous phase as an environment facilitating formation of secondary ions. The influence of the primary aerosol on the formation of secondary aerosol is out of the scope of this study, but merits further investigation to illustrate the mechanisms if there are influential effects.

3.3. Comparison of source contributions between APEC and non-EP-pre to evaluate the effects of control measures

To assess the effect of control measures taken during APEC, it is most reasonable to compare the periods between APEC and non-EP-pre which included days before and after APEC yet still before heating, eliminating the domestic heating period and the pollution episodes. Even though, the meteorological conditions during APEC were slightly less favorable. This is reflected in the following aspects: 1) There were a few shorter air mass trajectories through the polluted southwest area of Beijing during APEC (Fig. 2). Two short periods (episodes) with slightly elevated $PM_{2.5}$ level and organic carbon during APEC identified in previous studies (Chen et al., 2015; Sun et al., 2016) actually corresponded to these southern trajectories. 2) The WS was slightly lower during APEC (Fig. 1). 3) Some parameters (i.e. high RH and O_3 level) were more favorable for SIA formation during APEC (Fig. 1). Under these conditions, the following components showed significantly higher concentrations during APEC: $PM_{2.5}$ concentration (51.1 ± 50.2 vs 47.5 ± 59.5 μg m^{-3}), PAHs, alkanes, hopanes and anhydrosugers. The source contributions were higher for BB (5.8 ± 4.8 vs 3.4 ± 3.7 μg m^{-3}), traffic emission (6.5 ± 3.9 vs 4.9 ± 4.7 μg m^{-3}), comparable for industry emission (8.4 ± 13 vs 8.6 ± 8 μg m^{-3}) and lower for dust (2.2 ± 1.1 vs 3.1 ± 0.9 μg m^{-3}). Previous study has found uncontrolled random biomass/waste burning activity as an important $PM_{2.5}$ source during APEC (Yang et al., 2016). Despite the southern trajectories during APEC, the industry contribution was comparable, which is indicative of the effectiveness of control measures on industry emission. The effect of control measures on traffic emission seems to be less prominent and not as conclusive as for industry emissions, resulting in slightly higher contribution during APEC.

Note that previous studies mainly compared APEC period with adjacent periods before and/or after APEC, including pollution episodes. Applying a model approach, Liang et al. (2017b) found similar contributions of meteorological condition (30%) and control strategies (28%) to the reduction of $PM_{2.5}$ during APEC. In this study, APEC and non-EP-pre were both relative "clean" periods. By such a distinct approach of evaluation, the effectiveness of industry control measures was obvious. But this study also observed the limitation of such short term control measures under slightly unfavorable meteorological conditions. On the one hand, the controlled measures taken for traffic emission did not reduce the traffic contribution to the level of non-EP-pre period. On the other hand, the overall effect of control measures did not reduce the total $PM_{2.5}$ concentration to the level of "cleaner" period (non-EP-pre). Its effect was overwhelmed by other uncontrolled emissions and meteorological influence. This is also in line with the observation by Mao et al. (2018) that any control measure of PM emission had to overcome the substantial masking effect from variation of meteorological conditions to have a statistically detectable impact.

3.4. BaP_{eq} level and its relation to sources

BaP_{eq} is frequently used to assess the potential health risk of PAHs (Ren et al., 2019). And it is know that the PAH related toxicity in Beijing was much higher than many other big cities as also found in this study (Saha et al., 2017). The average BaP_{eq} during APEC, non-EP-pre, EP1 - EP 5, and non-EP-heat was 3.0 ± 2.4, 2.2 ± 2.4, 4.3 ± 0.3, 3.4 ± 1.6, 25.5 ± 12.9, 37.2 ± 22.9, 48.1 ± 17.4, 9.6 ± 10.2 ng m^{-3}, respectively. BaP_{eq} remained at comparably low levels in pre-heating period regardless of pollution episode as shown in Fig. 9. It increased significantly during heating period, resulting in more than 10 fold increase in health risk during heating episodes (EP3 - EP5). Therefore, huge short-term health effect existed during the heating episodes, which could put vulnerable people at very high risk. One more very important conclusion from this result is that even during the relative clean days of the heating period (non-EP-heat days), averagely 2-5 times higher BaP_{eq} level was observed as compared to pre-heating period. This result demonstrates the continuous long-term health risk during the heating-period, even though the low $PM_{2.5}$ concentration provides the feeling of "clean" and "safe" air. Yu et al. (2018) measured PAH concentrations before, during and after APEC periods in a rural area in the north of Beijing, and identified comparable BaP_{eq} level for APEC (3.69 ± 1.91 ng m^{-3}) and before APEC period (4.06 ± 2.65 ng m^{-3}). However, for the heating period after APEC, their daily sample measurement could not well track the variation during pollution episodes, and found the average during heating period was high (17.13 ± 3.21 ng m^{-3}). Ren et al. (2019) measured the BaP_{eq} during the 2015 China Victory Day Parade when control measures were taken and found much lower average level from August to September.

Fig. 9 also shows the average source contribution to BaP_{eq} of the defined periods to identify the major sources of BaP_{eq}. For EP3, EP4 and EP5 in the heating period, coal combustion was the largest BaP_{eq} contributor, while traffic made the second largest contribution. During pre-heating period, traffic became the dominating source of potential toxicity. Considering the actual value, BaP_{eq} toxicity contribution from coal combustion increased on average by a factor of over 10 comparing non-EP-heat to non-EP-pre even though the $PM_{2.5}$ mass was comparable under these two conditions, not to mention tremendous increase of its contribution by another factor of 3-6 during episodes comparing to non-episodes in the heating period. In total these would result in dozens of times of increase in BaP_{eq} of coal combustion source contribution during heating episodes comparing to pre-heating period. This highlights the importance of improving heating facilities, replacing heating fuels, and monitoring BaP in winter period. Not only in Beijing, but also in the northern part of China and other area where coal combustion is used quite a lot for domestic heating, it is relevant. Although strict measures have been taken to reduce coal emission in the Beijing area and in China, the coal is still the biggest source of heating in winter period and coal is still the main energy source. According the result of this study, this is indicative that the control measures is still far from sufficient for reducing coal combustion related health risk. In the study of (Yu et al., 2018), coal was the main contributor for BaP_{eq} before, during and after APEC. On the one hand, their sampling area was more rural, which could make a difference. On the other hand, they apportion the sources contributing to total PAH instead of $PM_{2.5}$, which is different from our method.

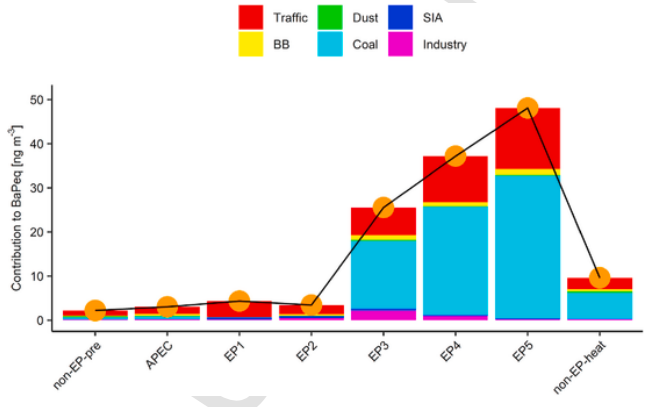

Fig. 9. The average contributions of different sources to BaP_{eq} (average value indicated by orange dots) in pollution episodes, APEC and non-episode. EP1 to EP5: episode 1 to episode 5, non-EP-pre: non-episode time during pre-heating period and non-EP-heat: non-episode time during heating period. BB: biomass burning; SIA: secondary inorganic aerosol. (For interpretation of the references to colour in this figure legend, the reader is referred to the Web version of this article.)

4. Conclusions

Using 6h high time resolution sampling in combination with sensitive organic analysis method, this study successfully tracked the variations of chemical species, particularly trace organic markers during the interesting autumn-winter transition period in Beijing. Especially, the variation during pollution episodes were well captured, which would not be possible with longer time off-line sampling normally needed for quantifying trace amount of organic species. Therefore, very reliable source apportionment studies were enabled through quantitative analysis of many source specific species as well as evaluation of diurnal variation. In addition, semi-quantitative source apportionment result in combination with quantitative PAH measurement further allowed the calculation of source specific BaP_{eq} toxicity contribution and the evaluation of the health risk from different sources under the atmospheric condition.

The findings of this study demonstrate the individual and combined effect of both emission sources and meteorological conditions, air mass trajectories on the PM level in Beijing area. The influences of both local and transported emissions are also shown. Firstly, coal combustion as a primary emission source was found to be highly related to domestic heating activity and temperature decrease in colder period. During heating period, coal combustion made tens of times more contribution to BaP_{eq} toxicity. This emphasizes the necessity of taking control measures to reduce not only short-term health effect during episodes but also long-term health effect even under low PM concentration in the heating period; not only in Beijing, but also other areas using coal for heating. Secondly, average SIA contribution decreased to 1/5 comparing non-EP-heat to non-EP-pre, and to 1/5-1/2 comparing episodes of heating period to pre-heating period. Whether this was mainly driven by decreased temperature and O_3 concentration or the substantial increase of organic species is still unclear. Further investigations are needed for studying the impact of organic aerosol components on SIA or even SOA formation. Thirdly, industry emission in the regional southern area was transported to Beijing as major industry source when air masses passed by the southern industry area, while traffic made bigger contribution with shorter and localized air mass trajectories. Industry emission was also most relevant with hazardous heavy metal pollution. Thes findings demonstrate the importance of regional improvement of air quality. Policy making should put more emphasis on the reduction of industry emission in general rather than focusing on decreasing polluted industry in one local area, i.e. relocating heavy polluted industries. Lastly, this study identified the effectiveness of control measures taken during APEC on reducing industry source contribution, while the effect on traffic emission was less clearly seen. And it was still not sufficiently effective to improve the overall air quality to the level under slightly more favorable meteorological conditions. This result pointed to the limitation of short term control measures on alleviating air pollution.

Credit roles

Fengxia Li?Writing - Original Draft, Writing - Review & Editing, Data preparation, Statistical analysis, Visualization, Investigation **Jianwei Gu:** Writing - Original Draft, Writing - Review & Editing, Data analysis, Investigation, Supervision **Jinyuan Xin**: Conceptualization, Funding acquisition, Supervision, Validation, Data curation, Editing **Juergen Schnelle-Kreis**: Conceptualization, Methodology, Writing - Original Draft, Writing - Review & Editing, Supervision, Project administration **Yuesi Wang**: Funding acquisition, Supervision, Conceptualization, Methodology **Zirui Liu**: Data curation, data Acquisition, Sampling, Data interpretation, Supervision **Rongrong Shen**: Sampling, Data acquisition and interpretation, Investigation **Bernhard Michalke**: Instrumental analysis, Data acquisition and interpretation, Supervision **Guelcin Abbaszade**: Instrumental analysis, Data acquisition, Investigation, Supervision **Ralf Zimmerman**: Conceptualization, Methodology, Supervision, Project administration.

Funding

This study was supported by the National Key Research and Development Program of China (grant number 2016YFC0202001), the Chinese Academy of Sciences Strategic Priority Research Program (grant number XDA23020301).

Declaration of competing interest

The authors declare that they have no known competing financial interests or personal relationships that could have appeared to influence the work reported in this paper.

Appendix A. Supplementary data

Supplementary data to this article can be found online at https://doi.org/10.1016/j.chemosphere.2021.130143.

References

Ansari, T.U., Wild, O., Li, J., Yang, T., Xu, W.Q., Sun, Y.L., Wang, Z.F., 2019. Effectiveness of short-term air quality emission controls: a high-resolution model study of Beijing during the Asia-Pacific Economic Cooperation (APEC) summit period. Atmos. Chem. Phys. 19, 8651–8668.

Bei, N.F., Li, X.P., Tie, X.X., Zhao, L.N., Wu, J.R., Li, X., Liu, L., Shen, Z.X., Li, G.H., 2020. Impact of synoptic patterns and meteorological elements on the wintertime haze in the Beijing-Tianjin-Hebei region, China from 2013 to 2017. Sci. Total Environ. 704, 12.

Chen, C., Sun, Y.L., Xu, W.Q., Du, W., Zhou, L.B., Han, T.T., Wang, Q.Q., Fu, P.Q., Wang, Z.F., Gao, Z.Q., Zhang, Q., Worsnop, D.R., 2015. Characteristics and sources of submicron aerosols above the urban canopy (260 m) in Beijing, China, during the 2014 APEC summit. Atmos. Chem. Phys. 15, 12879–12895.

Chen, J., Li, C., Ristovski, Z., Milic, A., Gu, Y., Islam, M.S., Wang, S., Hao, J., Zhang, H., He, C., Guo, H., Fu, H., Miljevic, B., Morawska, L., Thai, P., Lam, Y.F., Pereira, G., Ding, A., Huang, X., Dumka, U.C., 2017. A review of biomass burning: emissions and impacts on air quality, health and climate in China. Sci. Total Environ. 579, 1000–1034.

Cohen, A.J., Brauer, M., Burnett, R., Anderson, H.R., Frostad, J., Estep, K., Balakrishnan, K., Brunekreef, B., Dandona, L., Dandona, R., Feigin, V., Freedman, G., Hubbell, B., Jobling, A., Kan, H., Knibbs, L., Liu, Y., Martin, R., Morawska, L., Pope, C.A., III, Shin, H., Straif, K., Shaddick, G., Thomas, M., van Dingenen, R., van Donkelaar, A., Vos, T., Murray, C.J.L., Forouzanfar, M.H., 2017. Estimates and 25-year trends of the global burden of disease attributable to ambient air pollution: an analysis of data from the Global Burden of Diseases Study 2015. Lancet 389, 1907–1918.

Elser, M., Huang, R.J., Wolf, R., Slowik, J.G., Wang, Q.Y., Canonaco, F., Li, G.H., Bozzetti, C., Daellenbach, K.R., Huang, Y., Zhang, R.J., Li, Z.Q., Cao, J.J., Baltensperger, U., El-Haddad, I., Prevot, A.S.H., 2016. New insights into PM2.5 chemical composition and sources in two major cities in China during extreme haze events using aerosol mass spectrometry. Atmos. Chem. Phys. 16, 3207–3225.

Gao, J.J., Tian, H.Z., Cheng, K., Lu, L., Zheng, M., Wang, S.X., Hao, J.M., Wang, K., Hua, S.B., Zhu, C.Y., Wang, Y., 2015. The variation of chemical characteristics of PM2.5 and PM10 and formation causes during two haze pollution events in urban Beijing, China. Atmos. Environ. 107, 1–8.

Guo, S., Hu, M., Zamora, M.L., Peng, J.F., Shang, D.J., Zheng, J., Du, Z.F., Wu, Z., Shao, M., Zeng, L.M., Molina, M.J., Zhang, R.Y., 2014. Elucidating severe urban haze formation in China. Proc. Natl. Acad. Sci. U.S.A. 111, 17373–17378.

Han, B., Zhang, R., Yang, W., Bai, Z., Ma, Z., Zhang, W., 2016. Heavy haze episodes in Beijing during January 2013: inorganic ion chemistry and source analysis using highly time-resolved measurements from an urban site. Sci. Total Environ. 544, 319–329.

Han, L.H., Zhuang, G.S., Cheng, S.Y., Wang, Y., Li, J., 2007. Characteristics of re-suspended road dust and its impact on the atmospheric environment in Beijing. Atmos. Environ. 41, 7485–7499.

Hu, W.W., Hu, M., Hu, W., Jimenez, J.L., Yuan, B., Chen, W.T., Wang, M., Wu, Y.S., Chen, C., Wang, Z.B., Peng, J.F., Zeng, L.M., Shao, M., 2016. Chemical composition, sources, and aging process of submicron aerosols in Beijing: contrast between summer and winter. Journal of Geophysical Research-Atmospheres 121, 1955–1977.

Huang, R.-J., Zhang, Y., Bozzetti, C., Ho, K.-F., Cao, J.-J., Han, Y., Daellenbach, K.R., Slowik, J.G., Platt, S.M., Canonaco, F., Zotter, P., Wolf, R., Pieber, S.M., Bruns, E.A., Crippa, M., Ciarelli, G., Piazzalunga, A., Schwikowski, M., Abbaszade, G., Schnelle-Kreis, J., Zimmermann, R., An, Z., Szidat, S., Baltensperger, U., Haddad, I.E., Prévôt, A.S.H., 2014. High secondary aerosol contribution to particulate pollution during haze events in China. Nature 514, 218–222.

Huang, X.J., Liu, Z.R., Zhang, J.K., Wen, T.X., Ji, D.S., Wang, Y.S., 2016. Seasonal variation and secondary formation of size-segregated aerosol water-soluble inorganic ions during pollution episodes in Beijing. Atmos. Res. 168, 70–79.

Kanakidou, M., Seinfeld, J.H., Pandis, S.N., Barnes, I., Dentener, F.J., Facchini, M.C., Van Dingenen, R., Ervens, B., Nenes, A., Nielsen, C.J., Swietlicki, E., Putaud, J.P., Balkanski, Y., Fuzzi, S., Horth, J., Moortgat, G.K., Winterhalter, R., Myhre, C.E.L., Tsigaridis, K., Vignati, E., Stephanou, E.G., Wilson, J., 2005. Organic aerosol and global climate modelling: a review. Atmos. Chem. Phys. 5, 1053–1123.

Li, F., Schnelle-Kreis, J., Cyrys, J., Karg, E., Gu, J., Abbaszade, G., Orasche, J., Peters, A., Zimmermann, R., 2018a. Organic speciation of ambient quasi-ultrafine particulate matter (PM0.36) in Augsburg, Germany: seasonal variability and source apportionment. Sci. Total Environ. 615, 828–837.

Li, F., Schnelle-Kreis, J., Cyrys, J., Wolf, K., Karg, E., Gu, J., Orasche, J., Abbaszade, G., Peters, A., Zimmermann, R., 2018b. Spatial and temporal variation of sources contributing to quasi-ultrafine particulate matter PM0.36 in Augsburg, Germany. Sci. Total Environ. 631–632, 191–200.

Li, J., Han, Z., Li, J., Liu, R., Wu, Y., Liang, L., Zhang, R., 2020. The formation and evolution of secondary organic aerosol during haze events in Beijing in wintertime. Sci. Total Environ. 703, 134937.

Liang, P., Zhu, T., Fang, Y., Li, Y., Han, Y., Wu, Y., Hu, M., Wang, J., 2017a. The role of meteorological conditions and pollution control strategies in reducing air pollution in Beijing during APEC 2014 and Victory Parade 2015. Atmos. Chem. Phys. 17, 13921–13940.

Liang, P.F., Zhu, T., Fang, Y.H., Li, Y.R., Han, Y.Q., Wu, Y.S., Hu, M., Wang, J.X., 2017b. The role of meteorological conditions and pollution control strategies in reducing air pollution in Beijing during APEC 2014 and Victory Parade 2015. Atmos. Chem. Phys. 17.

Liu, Z.R., Gao, W.K., Yu, Y.C., Hu, B., Xin, J.Y., Sun, Y., Wang, L.L., Wang, G.H., Bi, X.H., Zhang, G.H., Xu, H.H., Cong, Z.Y., He, J., Xu, J.S., Wang, Y.S., 2018. Characteristics of PM2.5 mass concentrations and chemical species in urban and background areas of China: emerging results from the CARE-China network. Atmos. Chem. Phys. 18, 8849–8871.

Mao, L., Liu, R., Liao, W., Wang, X., Shao, M., Liu, S.C., Zhang, Y., 2018. An observation-based perspective of winter haze days in four major polluted regions of China. National Science Review 6, 515–523.

Nisbet, I.C.T., LaGoy, P.K., 1992. Toxic equivalency factors (TEFs) for polycyclic aromatic hydrocarbons (PAHs). Regul. Toxicol. Pharmacol. 16, 290–300.

Orasche, J., Schnelle-Kreis, J., Abbaszade, G., Zimmermann, R., 2011. Technical Note: in-situ derivatization thermal desorption GC-TOFMS for direct analysis of particle-bound non-polar and polar organic species. Atmos. Chem. Phys. 11, 8977–8993.

Pant, P., Harrison, R.M., 2012. Critical review of receptor modelling for particulate matter: a case study of India. Atmos. Environ. 49, 1–12.

Qi, J., Zheng, B., Li, M., Yu, F., Chen, C.C., Liu, F., Zhou, X.F., Yuan, J., Zhang, Q., He, K.B., 2017. A high-resolution air pollutants emission inventory in 2013 for the Beijing-Tianjin-Hebei region, China. Atmos. Environ. 170, 156–168.

Ren, H., Kang, M., Ren, L., Zhao, Y., Pan, X., Yue, S., Li, L., Zhao, W., Wei, L., Xie, Q., Li, J., Wang, Z., Sun, Y., Kawamura, K., Fu, P., 2018a. The organic molecular composition, diurnal variation, and stable carbon isotope ratios of PM2.5 in Beijing during the 2014 APEC summit. Environ. Pollut. 243, 919–928.

Ren, H., Kang, M.J., Ren, L.J., Zhao, Y., Pan, X.L., Yue, S.Y., Li, L.J., Zhao, W.Y., Wei, L.F., Xie, Q.R., Li, J., Wang, Z.F., Sun, Y.L., Kawamura, K., Fu, P.Q., 2018b. The organic molecular composition, diurnal variation, and stable carbon isotope ratios of PM2.5 in Beijing during the 2014 APEC summit. Environ. Pollut. 243, 919–928.

Ren, Y., Li, H., Meng, F., Wang, G., Zhang, H., Yang, T., Li, W., Ji, Y., Bi, F., Wang, X., 2019. Impact of emission controls on air quality in Beijing during the 2015 China Victory Day Parade: implication from organic aerosols. Atmos. Environ. 198, 207–214.

Saha, M., Maharana, D., Kurumisawa, R., Takada, H., Yeo, B.G., Rodrigues, A.C., Bhattacharya, B., Kumata, H., Okuda, T., He, K., Ma, Y., Nakajima, F., Zakaria, M.P., Giang, D.H., Viet, P.H., 2017. Seasonal trends of atmospheric PAHs in five asian megacities and source detection using suitable biomarkers. Aerosol and Air Quality Research 17, 2247–2262.

Samburova, V., Zielinska, B., Khlystov, A., 2013. Do 16 polycyclic aromatic hydrocarbons represent PAH air toxicity? Atmos. Chem. Phys. 13, 7053–7074.

Schnelle-Kreis, E., Sklorz, M., Peters, A., Cyrys, J., Zimmermann, R., 2005. Analysis of particle-associated semi-volatile aromatic and aliphatic hydrocarbons in urban particulate matter on a daily basis. Atmos. Environ. 39, 7702–7714.

Schnelle-Kreis, J., Sklorz, M., Orasche, J., Stoelzel, M., Peters, A., Zimmermann, R., 2007. Semi volatile organic compounds in ambient PM(2.5). Seasonal trends and daily resolved source contributions. Environ. Sci. Technol. 41, 3821–3828.

Shao, P.Y., Tian, H.Z., Sun, Y.J., Liu, H.J., Wu, B.B., Liu, S.H., Liu, X.Y., Wu, Y.M., Liang, W.Z., Wang, Y., Gao, J.J., Xue, Y.F., Bai, X.X., Liu, W., Lin, S.M., Hu, G.Z., 2018. Characterizing remarkable changes of severe haze events and chemical compositions in multi-size airborne particles (PM1, PM2.5 and PM10) from January 2013 to 2016-2017 winter in Beijing, China. Atmos. Environ. 189, 133–144.

Simoneit, B.R.T., Schauer, J.J., Nolte, C.G., Oros, D.R., Elias, V.O., Fraser, M.P., Rogge, W.F., Cass, G.R., 1999. Levoglucosan, a tracer for cellulose in biomass burning and atmospheric particles. Atmos. Environ. 33, 173–182.

Sun, Y., Wang, Z., Dong, H., Yang, T., Li, J., Pan, X., Chen, P., Jayne, J.T., 2012. Characterization of summer organic and inorganic aerosols in beijing, China with an aerosol chemical speciation monitor. Atmos. Environ. 51, 250–259.

Sun, Y., Wang, Z., Wild, O., Xu, W., Chen, C., Fu, P., Du, W., Zhou, L., Zhang, Q., Han, T., Wang, Q., Pan, X., Zheng, H., Li, J., Guo, X., Liu, J., Worsnop, D.R., 2016. "APEC blue": secondary aerosol reductions from emission controls in beijing. Sci. Rep. 6, 20668.

Sun, Y.L., Wang, Z.F., Du, W., Zhang, Q., Wang, Q.Q., Fu, P.Q., Pan, X.L., Li, J., Jayne, J., Worsnop, D.R., 2015. Long-term real-time measurements of aerosol particle composition in Beijing, China: seasonal variations, meteorological effects, and source analysis. Atmos. Chem. Phys. 15, 10149–10165.

Sun, Y.L., Zhuang, G.S., Tang, A.H., Wang, Y., An, Z.S., 2006. Chemical characteristics of PM2.5 and PM10 in haze-fog episodes in Beijing. Environ. Sci. Technol. 40, 3148–3155.

Tan, J.H., Duan, J.C., Zhen, N.J., He, K.B., Hao, J.M., 2016. Chemical characteristics and source of size-fractionated atmospheric particle in haze episode in Beijing. Atmos. Res. 167, 24–33.

Tan, T.Y., Hu, M., Li, M.R., Guo, Q.F., Wu, Y.S., Fang, X., Gu, F.T., Wang, Y., Wu, Z.J., 2018. New insight into PM2.5 pollution patterns in Beijing based on one-year measurement of chemical compositions. Sci. Total Environ. 621, 734–743.

Thurston, G.D., Spengler, J.D., 1985. A quantitative assessment of source contributions to inhalable particulate matter pollution in metropolitan Boston. Atmos. Environ. 19, 9–25 1967.

Tian, S.L., Pan, Y.P., Wang, Y.S., 2016. Size-resolved source apportionment of particulate matter in urban Beijing during haze and non-haze episodes. Atmos. Chem. Phys. 16, 1–19.

UN Environment, 2019. A Review of 20 Years' Air Pollution Control in Beijing. United Nations Environment Programme, Nairobi, Kenya.

Wang, Q., Shao, M., Zhang, Y., Wei, Y., Hu, M., Guo, S., 2009. Source apportionment of fine organic aerosols in Beijing. Atmos. Chem. Phys. 9, 8573–8585.

Wang, Y.Q., Zhang, Y., Schauer, J.J., de Foy, B., Guo, B., Zhang, Y.X., 2016. Relative impact of emissions controls and meteorology on air pollution mitigation associated with the Asia-Pacific Economic Cooperation (APEC) conference in Beijing, China. Sci. Total Environ. 571, 1467–1476.

Wang, Y.S., Yao, L., Wang, L.L., Liu, Z.R., Ji, D.S., Tang, G.Q., Zhang, J.K., Sun, Y., Hu, B., Xin, J.Y., 2014. Mechanism for the formation of the January 2013 heavy haze pollution episode over central and eastern China. Sci. China Earth Sci. 57, 14–25.

Xu, W., Liu, X.J., Liu, L., Dore, A.O., Tang, A.H., Lu, L., Wu, Q.H., Zhang, Y.Y., Hao, T.X., Pan, Y.P., Chen, J.M., Zhang, F.S., 2019. Impact of emission controls on air quality in Beijing during APEC 2014: implications from water-soluble ions and carbonaceous aerosol in PM2.5 and their precursors. Atmos. Environ. 210, 241–252.

Yang, H., Chen, J., Wen, J., Tian, H., Liu, X., 2016. Composition and sources of PM2.5 around the heating periods of 2013 and 2014 in Beijing: implications for efficient mitigation measures. Atmos. Environ. 124, 378–386.

Yang, S., Duan, F.K., Ma, Y.L., Li, H., Ma, T., Zhu, L.D., Huang, T., Kimoto, T., He, K.B., 2020. Mixed and intensive haze pollution during the transition period between autumn and winter in Beijing, China. Sci. Total Environ. 711, 10.

Yang, Y.R., Liu, X.G., Qu, Y., An, J.L., Jiang, R., Zhang, Y.H., Sun, Y.L., Wu, Z.J., Zhang, F., Xu, W.Q., Ma, Q.X., 2015a. Characteristics and formation mechanism of continuous hazes in China: a case study during the autumn of 2014 in the North China Plain. Atmos. Chem. Phys. 15, 8165–8178.

Yang, Y.R., Liu, X.G., Qu, Y., An, J.L., Jiang, R., Zhang, Y.H., Sun, Y.L., Wu, Z.J., Zhang, F., Xu, W.Q., Ma, Q.X., 2015b. Characteristics and formation mechanism of continuous hazes in China: a case study during the autumn of 2014 in the North China Plain. Atmos. Chem. Phys. 15, 8165–8178.

Yang, Y.R., Liu, X.G., Qu, Y., Wang, J.L., An, J.L., Zhang, Y., Zhang, F., 2015c. Formation mechanism of continuous extreme haze episodes in the megacity Beijing, China, in January 2013. Atmos. Res. 155, 192–203.

Yu, Q., Yang, W., Zhu, M., Gao, B., Li, S., Li, G., Fang, H., Zhou, H., Zhang, H., Wu, Z., Song, W., Tan, J., Zhang, Y., Bi, X., Chen, L., Wang, X., 2018. Ambient PM2.5-bound polycyclic aromatic hydrocarbons (PAHs) in rural Beijing: unabated with enhanced temporary emission control during the 2014 APEC summit and largely aggravated after the start of wintertime heating. Environ. Pollut. 238, 532–542.

Zhang, R., Jing, J., Tao, J., Hsu, S.C., Wang, G., Cao, J., Lee, C.S.L., Zhu, L., Chen, Z., Zhao, Y., Shen, Z., 2013. Chemical characterization and source apportionment of $PM_{2.5}$ in Beijing: seasonal perspective. Atmos. Chem. Phys. 13, 7053–7074.

Zhang, R., Sun, X.S., Shi, A.J., Huang, Y.H., Yan, J., Nie, T., Yan, X., Li, X., 2018. Secondary inorganic aerosols formation during haze episodes at an urban site in Beijing, China. Atmos. Environ. 177, 275–282.

Zhang, Y.X., Schauer, J.J., Zhang, Y.H., Zeng, L.M., Wei, Y.J., Liu, Y., Shao, M., 2008. Characteristics of particulate carbon emissions from real-world Chinese coal combustion. Environ. Sci. Technol. 42, 5068–5073.

Zhao, X.J., Zhao, P.S., Xu, J., Meng, W., Pu, W.W., Dong, F., He, D., Shi, Q.F., 2013. Analysis of a winter regional haze event and its formation mechanism in the North China Plain. Atmos. Chem. Phys. 13, 5685–5696.

Zheng, G.J., Duan, F.K., Su, H., Ma, Y.L., Cheng, Y., Zheng, B., Zhang, Q., Huang, T., Kimoto, T., Chang, D., Poschl, U., Cheng, Y.F., He, K.B., 2015. Exploring the severe winter haze in Beijing: the impact of synoptic weather, regional transport and heterogeneous reactions. Atmos. Chem. Phys. 15, 2969–2983.

Zhu, Y., Huang, L., Li, J., Ying, Q., Zhang, H., Liu, X., Liao, H., Li, N., Liu, Z., Mao, Y., Fang, H., Hu, J., 2018. Sources of particulate matter in China: insights from source apportionment studies published in 1987–2017. Environ. Int. 115, 343–357.